Hearing Research 332 (2016) 29–38

Contents lists available at ScienceDirect

Hearing Research

journal homepage: www.elsevier.com/locate/heares

Research paper

# The middle ear muscle reflex in the diagnosis of cochlear neuropathy

Michelle D. Valero [a, b, *], Kenneth E. Hancock [a, b], M. Charles Liberman [a, b]

[a] Eaton-Peabody Laboratories, Massachusetts Eye and Ear Infirmary, Boston, MA 02114, USA
[b] Department of Otology and Laryngology, Harvard Medical School, Boston, MA 02115, USA

ARTICLE INFO

*Article history:*
Received 6 October 2015
Received in revised form
14 November 2015
Accepted 17 November 2015
Available online 30 November 2015

*Keywords:*
Cochlear neuropathy
Hidden hearing loss
Acoustic overexposure
Middle-ear muscle reflex
Medial olivocochlear reflex
Wideband reflectance

ABSTRACT

Cochlear neuropathy, i.e. the loss of auditory nerve fibers (ANFs) without loss of hair cells, may cause hearing deficits without affecting threshold sensitivity, particularly if the subset of ANFs with high thresholds and low spontaneous rates (SRs) is preferentially lost, as appears to be the case in both aging and noise-damaged cochleas. Because low-SR fibers may also be important drivers of the medial olivocochlear reflex (MOCR) and middle-ear muscle reflex (MEMR), these reflexes might be sensitive metrics of cochlear neuropathy. To test this hypothesis, we measured reflex strength and reflex threshold in mice with noise-induced neuropathy, as documented by confocal analysis of immunostained cochlear whole-mounts. To assay the MOCR, we measured contra-noise modulation of ipsilateral distortion-product otoacoustic emissions (DPOAEs) before and after the administration of curare to block the MEMR or curare + strychnine to also block the MOCR. The modulation of DPOAEs was 1) dominated by the MEMR in anesthetized mice, with a smaller contribution from the MOCR, and 2) significantly attenuated in neuropathic mice, but only when the MEMR was intact. We then measured MEMR growth functions by monitoring contra-noise induced changes in the wideband reflectance of chirps presented to the ipsilateral ear. We found 1) that the changes in wideband reflectance were mediated by the MEMR alone, and 2) that MEMR threshold was elevated and its maximum amplitude was attenuated in neuropathic mice. These data suggest that the MEMR may be valuable in the early detection of cochlear neuropathy.

Published by Elsevier B.V.

## 1. Introduction

Auditory neuropathy is defined clinically by normal OAEs with an absent or grossly abnormal ABR. There are likely numerous etiologies, but in such patients, outer hair cells (OHCs) must be functioning normally, while auditory nerve fibers (ANFs) and/or inner hair cells (IHCs) are presumably absent or dysfunctional. Some patients with auditory neuropathy have normal audiometric thresholds, but extreme difficulty understanding speech even in a quiet environment (Starr et al., 1996). In such cases, the degree of nerve loss/dysfunction must be extreme, and in such patients the MEMR is often absent (Berlin et al., 2005).

Recent work in animals shows that noise exposures that do not permanently damage hair cells can nevertheless cause a permanent partial loss of auditory-nerve peripheral synapses (Kujawa and Liberman, 2009; Liberman et al., 2015). This more moderate type of neuropathy results in a "hidden hearing loss," in which cochlear thresholds, as assayed by either auditory brainstem responses (ABRs) or otoacoustic emissions (OAEs), fully recover, but suprathreshold amplitudes of the ABR wave I, which represent the summed activity of auditory nerve fibers, are permanently reduced. This disconnect between threshold and suprathreshold pathophysiology arises because the noise preferentially damages the subset of auditory nerve fibers with higher thresholds and lower spontaneous firing rates (low- and medium-SR fibers), which constitute ~40% of the auditory nerve population (Furman et al., 2013).

This type of cochlear neuropathy is an important component of age-related hearing loss (Sergeyenko et al., 2013), noise-induced hearing loss (Kujawa and Liberman, 2009), and other types of acquired sensorineural hearing loss (e.g., Ruan et al., 2014). Behavioral audiograms can remain unaffected by neuropathy until it is near-total (~80–90%) thanks to the redundancy of IHC innervation (Schuknecht and Woellner, 1955; Lobarinas et al., 2013). However, more moderate neuropathies, while unlikely to cause perceptual impairment as profound as classic auditory neuropathy, are likely to cause significant deficits in hearing-in-noise, particularly if low-

* Corresponding author. Eaton Peabody Laboratories, Massachusetts Eye and Ear Infirmary, 243 Charles Street, Boston, MA 02114, USA.
*E-mail address:* Michelle_Valero@meei.harvard.edu (M.D. Valero).

http://dx.doi.org/10.1016/j.heares.2015.11.005
0378-5955/Published by Elsevier B.V.

SR fibers are preferentially lost, due to the relative insensitivity of low-SR fibers to masking by continuous noise (Costalupes et al., 1984).

Low-SR afferents may also be important drivers of the medial olivocochlear reflex (MOCR: Liberman, 1988, 1991; Ye et al., 2000) and the middle-ear muscle reflex (MEMR: Liberman and Kiang, 1984; Roullier et al., 1986; Kobler et al., 1992). These reflexes can reduce the sound-evoked excitation of inner hair cells by either decreasing the gain of the cochlear amplifier, as is the case for the MOCR, or increasing the impedance of the middle ear, as is the case for the MEMR. The effective stimulus attenuation from either reflex can protect the cochlea from damaging sounds (MEMR: Simmons, 1960; Borg, 1966; MOCR: Rajan, 1995; Reiter and Liberman, 1995). A trauma-induced impairment of the reflexes may initiate a vicious cycle wherein reduced reflex strength worsens cochlear damage, which further reduces the strength of the negative feedback, which may ultimately lead to hair cell loss and permanent threshold shifts (Wang and Ren, 2012). Furthermore, because both MOC and MEM reflexes can enhance signal detection in noise (e.g., Kawase et al., 1993; Pang and Guinan, 1997; respectively), their weakening could exacerbate any hearing-in-noise and word-recognition deficits arising from a loss of low-SR fibers.

Neurotrophin overexpression can repair noise-induced neuropathy in transgenic mice (Wan et al., 2014), but a major impediment to the application of neurotrophin therapies to humans is the inability to diagnose this subtotal primary neural degeneration. The amplitude of ABR wave I is a useful indicator of neuropathy in animals and has been shown to scale well with synaptic loss as documented in post-mortem histopathology (Kujawa and Liberman, 2009; Furman et al., 2013). However, although group differences in the ABR wave-I amplitude can be detected in humans (e.g., Schaette and McAlpine, 2011), they are highly variable in the clinic, which may limit their diagnostic utility (Gorga et al., 1988; Nikiforidis et al., 1993). The envelope-following response may be a more robust diagnostic tool (Plack et al., 2014; Shaheen et al., 2015), but a battery of short-duration tests may be most useful in differential diagnoses.

If the MOC and MEM reflexes are driven by the low- and medium-SR fibers that are selectively destroyed in cochlear neuropathy, then some measure of reflex strength might serve as a useful, non-invasive, and objective assay to aid in the detection of hidden hearing loss in humans. In the present study, we tested this hypothesis by measuring MOC and MEM reflexes in anesthetized mice with noise-induced cochlear neuropathy.

## 2. Materials and methods

### 2.1. Animals and groups

Male CBA/CaJ mice were used in this study. Group 1 (n = 12) mice were received at 6 wks. At 7 wks, half the animals were exposed to neuropathic noise. Cochlear function tests (see below) were measured 2 wks post exposure, and at least 2 days after that, contra-noise modulation of DPOAEs was measured. The cochleas were then harvested from a subset of exposed and control mice for histological analysis. Group 2 (n = 8) mice were received at 10 wks. At 16 wks, half were exposed to neuropathic noise. Cochlear function and contra-noise modulation of wideband acoustic reflectance was measured at 24 h, and 1, 2, 4, and 8 wks post exposure. The cochleas were then harvested for histological analysis. When required, curare alone or curare with strychnine was injected intramuscularly at 4 mg/kg and 10 mg/kg, respectively, after tracheostomy and mechanical ventilation. For all physiological measurements, mice were anesthetized with ketamine (100 mg/kg) and xylazine (20 mg/kg) and placed inside an electrically and acoustically shielded room maintained at 30 °C. Heart rate was monitored via the ABR electrodes. Booster injections (1/3 of the original dose) were given when whisking-related noise was observed on the ABR trace, which was typically 30–45 min following the last injection. Curarized animals were given boosters at 30 min intervals. All procedures were approved by the Animal Care and Use Committee at the Massachusetts Eye and Ear Infirmary.

### 2.2. Noise exposure

Awake mice were placed unrestrained inside a mesh container within a reverberant chamber and were presented with spectrally flattened, octave-band noise (8–16 kHz) for two hours. The SPLs were 97.5 and 99 dB SPL for Group 1 and Group 2, respectively.

### 2.3. Stimulus calibration

Acoustic systems were regularly calibrated in a small custom coupler by comparing the output voltage of the probe tube microphone to that of a calibrated ¼ condenser microphone (Larsen-Davis Type 2530). For each subject and each placement of the acoustic system, the ear-canal SPL was calibrated with a moderate-level chirp stimulus to determine the transducer voltage required to produce the target SPLs.

### 2.4. Cochlear function tests

For DPOAEs, $f_1$ and $f_2$ primary tones ($f_2/f_1 = 1.2$) were presented with $f_2$ varied between 5.6 and 45.2 kHz in half-octave steps and $L_1-L_2 = 10$ dB. At each $f_2$, $L_2$ was varied between 10 and 80 dB SPL in 10-dB increments. DPOAE threshold was defined as the $L_2$-level eliciting a DPOAE of magnitude 5 dB SPL. Stimuli were generated with 24-bit digital I–O cards (National Instruments PXI-4461) in a PXI-1042Q chassis, amplified by an SA-1 speaker driver (Tucker–Davis Technologies, Inc.), and delivered from two electrostatic drivers (CUI CDMG15008-03A) in our custom acoustic system. An electret microphone (Knowles FG-23329-P07) at the end of a small probe tube was used to monitor ear-canal sound pressure. For ABRs, tone pips (5-msec duration, 0.5-msec ramp) were presented in alternating polarity at 40 Hz using the acoustic assembly described above. At each test frequency (5.6–45.2 kHz in 1/2-octave steps), stimulus levels were incremented from 10 to 80 dB SPL. Responses were measured from needle electrodes in vertex-to-pinna configuration with the ground just above the tail. A Grass pre-amplifier (Model P511) amplified (10,000X) and band-pass filtered (0.3–3 kHz) the ABR waveforms. 1024 artifact-free waveforms (512 of each polarity) were averaged to produce the final ABR trace. Threshold was defined by visual inspection of the stacked waveforms. Wave-I amplitude was defined as the difference between the maximum of the peak and the minimum of the subsequent trough.

### 2.5. Modulation of DPOAEs by contralateral noise (group 1)

DPOAE-eliciting stimuli were presented to the ipsilateral ear at $f_2 = 32$ kHz ($f_2/f_1 = 1.2$). First, DPOAEs were measured in a 13 × 13 level-matrix (1-dB resolution) with primary tones presented continuously for 0.5 sec at each $L_1$-$L_2$ combination. Then, a 6 × 6 level matrix, centered at the appropriate $L_1$-$L_2$ combination (see Results), was measured in 1-dB resolution. For the second matrix, primary tones were presented continuously for 7 sec at each $L_1$-$L_2$ combination, and the contralateral noise was presented during the 6th second (5-msec ramp). The contralateral noise was spectrally flattened, 2 octave-band noise centered at $f_2$ and presented at 95 dB SPL. A 5-sec period of silence was interposed between each level step.

### 2.6. Modulation of wideband acoustic reflectance by contralateral noise (group 2)

Ipsilateral stimuli (probes) were 80 dB SPL, 2-msec Hanning-windowed "chirps," upswept from 4 to 64 kHz and presented at 40 Hz. The phase spectrum was adjusted to compensate for the effect of the Hanning window, yielding a chirp with a flat magnitude spectrum (Neumann et al., 1994). Two seconds following the onset of the "chirp train," the contralateral noise (reflex elicitor) was presented for 1 sec (20-msec ramp). The elicitor was high-pass (16–45.2 kHz), spectrally flattened, frozen noise. Each 6-sec chirp train was presented in two contiguous trials with the elicitor presented once in each trial in alternating polarity to eliminate any acoustic cross-talk from the contra noise. The sound pressure waveform in the ipsilateral ear canal was averaged over corresponding time points from the two 6-sec trials, and the spectrum was computed separately for the average chirp waveform before vs. during the elicitor presentation. The elicitor was then incremented from 72 to 100 dB in 2-dB steps. See text for further details.

### 2.7. Cochlear immunostaining

Mice were perfused intracardially with 4% paraformaldehyde (PFA) for 5 min, after which the cochleas were exposed and perfused with 4% PFA after opening the oval and round windows. The perfused cochleas were extracted, post-fixed for 2 hr in 4% PFA, and decalcified in EDTA for 48 hr at room temperature. They were then dissected into half-turns and incubated in primary antibodies: 1) mouse (IgG1) anti-CtBP2 from BD Transduction Labs at 1:200 and 2) mouse (IgG2) anti-GluA2 from Millipore at 1:2000. Primary incubations were followed by 1-hr incubations in species-appropriate secondary antibodies.

### 2.8. Innervation analysis and hair cell counts

Cochlear lengths and a frequency-place map were obtained for each case from micrographs of dissected pieces using an image J plugin (http://www.masseyeandear.org/research/ent/eatonpeabody/epl-histology-resources/). Confocal z-stacks were collected using a 100× oil-immersion objective (N.A. = 1.4) and 2× digital zoom on a Leica TCS SP2 confocal at cochlear frequency locations corresponding to the physiological assays. Synapses in the IHC area were counted using Amira (Visage Imaging) to find the xyz coordinates of all the ribbons (CtBP2-positive puncta), and custom re-projection software was then used to assess the fraction of ribbons with closely apposed glutamate-receptor patches (i.e. GluA2 puncta). OHCs were counted under DIC microscopy with a Nikon Eclipse E800 microscope following confocal analyses.

### 2.9. Statistical analyses

Statistics were performed in Kaleidagraph (Synergy Software) or MATLAB. Two-way repeated-measure ANOVAs adjusted with the Holm-Bonferroni correction were used to assess the significance of group differences.

## 3. Results

### 3.1. Verifying noise-induced cochlear neuropathy

The first group of 7-wk old mice was exposed to noise (8–16 kHz) at 97.5 dB SPL for 2 hr. This exposure caused an acute threshold shift of ~40 dB when measured 24 hr post-exposure (see Kujawa and Liberman, 2015). When measured 2 wk post-exposure, ABR thresholds recovered to baseline at all but the highest frequency (Fig. 1B), and DPOAE thresholds recovered at all frequencies (Fig. 1E). Despite the nearly complete threshold recovery, suprathreshold ABR wave-I amplitudes were decreased by 40–50% at 32 and 45 kHz (Fig. 1C), while suprathreshold DPOAE amplitudes recovered to control values at all but the highest frequency (Fig. 1F).

In hopes of producing a more completely reversible threshold elevation, even at the highest test frequencies, we exposed a second group of mice at 16 wks of age, when they are slightly less vulnerable (Kujawa and Liberman, 2006). 24 hr following exposure, ABR and DPOAE thresholds were elevated by > 40 dB at 32 kHz (Fig. 1B,E). Indeed, thresholds measured 2 wk later had recovered completely at all test frequencies. Once again, the suprathreshold wave-I amplitudes were reduced by up to 40% at high frequencies (Fig. 1C), while the DPOAE suprathreshold amplitudes recovered at all frequencies (Fig. 1E).

The histopathology was consistent with that observed in previous studies of cochlear neuropathy (e.g., Kujawa and Liberman, 2009; Liberman et al., 2015; Shaheen et al., 2015): the number of synapses was reduced by 40–50% in the basal half of the cochlea (Fig. 1A), while there was no loss of IHCs anywhere in the cochlea (not shown). OHCs remained intact at all cochlear regions except the extreme basal tip (Fig. 1D).

### 3.2. Contra-noise modulation of DPOAEs

We first aimed to measure the effects of noise-induced cochlear neuropathy on MOC reflex strength using the modulation of ipsilateral DPOAEs by contralateral noise (e.g., Collet et al., 1990). Because MOC efferents lower the gain of the cochlear amplifier, and because the cochlear amplifier effects are strongest at low SPLs, contra-sound modulation of DPOAEs is typically greatest at low ipsilateral stimulus levels (see Guinan, 2006). However, in mice, contra-sound effects on low-level DPOAEs are greatly reduced by anesthesia (Chambers et al., 2012), and the remaining suppression is not mediated by the MOC system (Maison et al., 2012). When elicited with high-level primary tones, DPOAEs saturate, and MOC activation elicits only small changes in DPOAE amplitude. However, the MOC-mediated modulation of high-level DPOAEs can be magnified around the non-monotonicity, or "notch," in the amplitude vs. level function, which occurs at primary-tone levels between 70 and 90 dB SPL (Kujawa and Liberman, 2001). When MOC effects are measured around this notch, DPOAE enhancement or suppression can be observed, depending on whether primary-tone levels are below or above the notch.

In mice, the notch is robust when $f_2$ is at 32 kHz (Fig. 2A), the frequency of maximal synaptic damage (Fig. 1). Because notch depth is sensitive to the $L_1$-$L_2$ combination, prior studies have measured contra-noise effects for a matrix of ipsilateral $L_1$-$L_2$ combinations (Kujawa and Liberman, 2001; Maison et al., 2012). Adopting that approach, we measured DPOAE amplitude in 1-dB increments of $L_1$ and $L_2$ (Fig. 2B). Notches were always present, and the primary levels needed to elicit them overlapped in exposed and control ears (Fig. 2C). $L_1$ and $L_2$ primary tones were presented in a 6 × 6 level matrix (1-dB increments) centered on the notch (Fig. 2E), and at each of the 36 $L_1$-$L_2$ combinations, the change in DPOAE amplitude was measured during a 1-sec contra-noise presentation (Fig. 2D). The maximum contra-noise enhancement was seen exactly at the $L_1$-$L_2$ combination evoking the deepest notch (Fig. 2F vs. E). Identical measurements made ~45 min post-mortem (not shown) revealed no system distortion at $2f_1-f_2$: with $L_1$-$L_2$ ranging from 81/80–93/92, the mean (SD) amplitude at $2f_1-f_2$ was −7.6 (2.27) dB SPL.

In control mice, mean contra-noise enhancement and suppression were ~10 dB (Fig. 3A). To rule out acoustic crosstalk, we measured contra-noise effects before and after removal of the

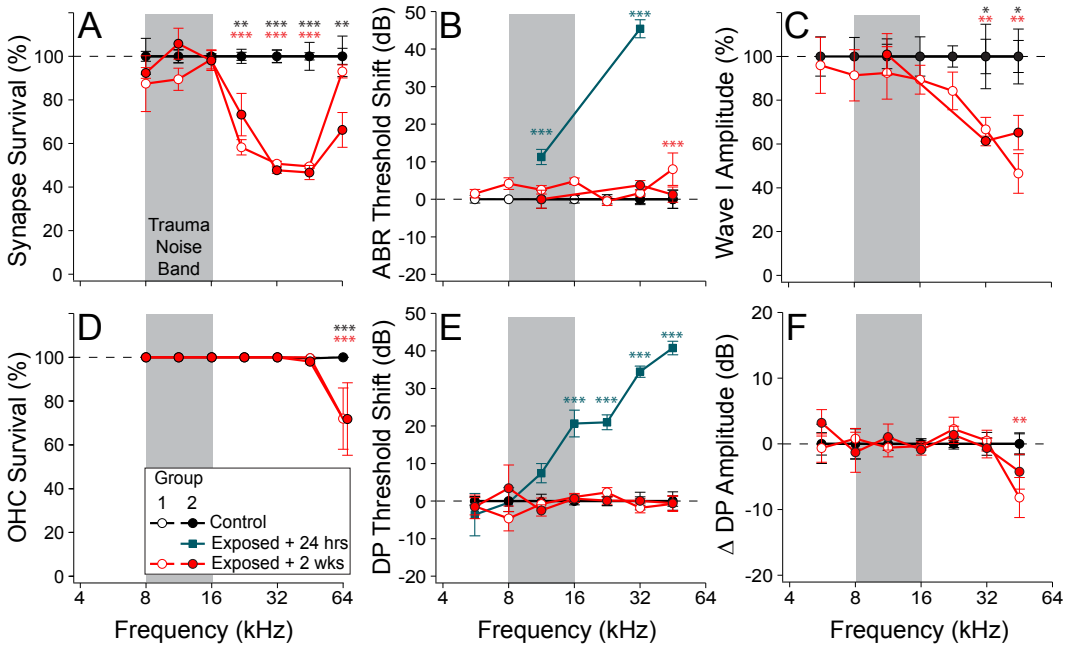


**Fig. 1.** Effects of neuropathic noise on cochlear synapses, OHCs, threshold and suprathreshold responses. A,D: Mean survival of IHC synapses and OHCs, respectively, for the two groups of noise-exposed animals. B,E: Mean threshold shifts as measured by ABRs or DPOAEs, respectively, at either 24 hr (teal) or 2 wk (red) post-exposure. C,F: Mean suprathreshold amplitudes for ABR wave I and DPOAEs, respectively. In each ear, for each measure, response amplitudes were averaged across stimulus levels of 60–80 dB SPL. All values in all panels are normalized to mean values for two groups of unexposed, age-matched controls. Error bars indicate SEM. Symbol key in D applies to all panels. Asterisks indicate statistical significance: * for $P < 0.05$; ** for $P < 0.01$; *** for $P < 0.001$. Red asterisks refer to Group 1. Black and teal asterisks refer to Group 2.

contralateral tympanic membrane: the effects disappeared (Fig. 3C). To determine the contribution of the MEMR to this effect, we injected curare at a dose that paralyzes striated muscles, including the MEMs, but has no effect on the MOC system (Elgoyhen et al., 1994; Maison et al., 2012). Curarization significantly attenuated the effect, suggesting that the MEMR dominates the contra-noise modulations of high-level DPOAEs in the anesthetized mouse. Consistent with MEM activation, the ear-canal SPL of the primary-tones shifted during the contralateral noise (Fig. 3B). Although the shift was tiny (usually < 0.1 dB), it was reproducible and always disappeared after curare (Fig. 3B). To determine whether the small contra-noise effect seen after curarization was mediated by the MOC reflex, we added strychnine, a potent antagonist at the $\alpha 9/\alpha 10$ nicotinic acetylcholine receptor through which MOC terminals inhibit OHC amplification (Elgoyhen et al., 2001; Rothlin et al., 1999; Sridhar et al., 1995). Following strychnine, no contra-noise modulations of DPOAEs could be measured (Fig. 3A, green).

With both the MOC and the MEM reflexes intact, the contra-noise modulation of DPOAEs was significantly attenuated in neuropathic mice when compared to age-matched controls (Fig. 4A). However, after inactivating the MEM with curare, the small remaining modulations were not significantly affected by neuropathy (Fig. 4B).

### 3.3. Contra-noise modulation of wideband acoustic reflectance

Given that contra-noise effects in the ketamine/xylazine-anesthetized mouse seemed to be dominated by MEMs, and given that the effect was significantly weakened in neuropathic mice, we aimed to design an assay better suited to study this MEMR. In the clinic, the contralateral MEMR is studied by measuring contra-sound evoked changes in the sound pressure of a low-frequency (<1 kHz) probe tone presented to the ipsilateral ear canal. However, the MEMR threshold is dependent on the frequency of both probe tone and contralateral reflex elicitor (McMillan et al., 1985). By using a wideband probe, like those utilized in measurements of wideband acoustic reflectance (e.g., Keefe et al., 1992; Feeney and Keefe, 2001), the effect of the MEMR on a wide frequency range could be examined. In the present study, the contra-noise mediated change in SPL was used as a proxy for reflectance, although the relationship between the two is dependent upon several variables not considered here (see Rosowski et al., 2013 for a review). Because MEMRs have not previously been measured in mice, and because the DPOAE assay suggested that the MEMR could modify the reflectance of tones as high in frequency as 32 kHz, the passband of the chirp (4–64 kHz) was set to cover nearly the full audible range of the mouse. The use of high-level (80 dB SPL) ipsilateral chirps (Schairer et al., 2013) minimized contamination of the ear-canal SPL by stimulus-frequency OAEs (Guinan et al., 2003).

With respect to the contralateral noise, broadband elicitors can elicit the MEMR at lower intensities than pure tones (e.g. Margolis, 1993; Feeney and Keefe, 2001; Feeney et al., 2003, 2004), and they are more sensitive to cochlear pathology (Popelka et al., 1976; Gelfand and Piper, 1981; Gelfand et al., 1983). Here, the pass-band of the reflex elicitor (Fig. 5B, gray shaded area) was set to cover cochlear frequencies where neuropathy was maximal and OHCs were intact (Fig. 1A, D).

As observed for DPOAE-eliciting primary tones (Fig. 3B), contralateral noise modulated the SPL of the chirps in the ipsilateral ear canal. This modulation of SPL was due to a change in reflectance at the tympanic membrane. We averaged waveforms separately for chirps presented with vs. without contralateral noise, then fast Fourier-transformed each mean waveform and plotted the contra-noise effect as the difference between the two magnitude spectra (Fig. 5B). The complex frequency dependence of the effect was reminiscent of wideband reflectance measured in humans (e.g.,

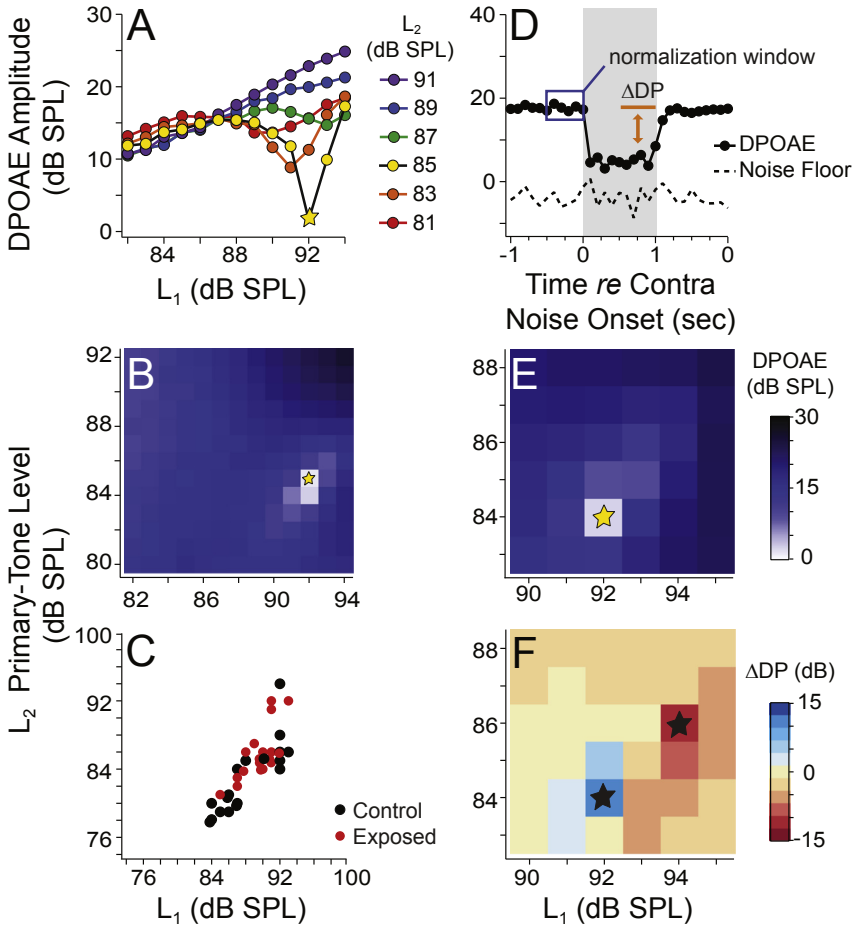


**Fig. 2.** Measuring contra-noise modulation of high-level DPOAEs near the notch in the amplitude vs. level function. A,B: DPOAEs were measured with 13 $L_1$ and 13 $L_2$ values incremented in 1-dB steps. The DPOAE amplitude at each $L_1$-$L_2$ combination in the level matrix was plotted as a heat map (B), and a subset of these functions are shown as amplitude vs. level functions (A). The functions have a prominent notch at high SPLs, and the center of the notch is marked with a yellow star in A and B. C: The location of notch center in the $L_1$-$L_2$ space varied between and within animals, but did not differ much between control and exposed groups. D: A 6 × 6 dB level matrix was focused around notch center, and the effect of contralateral noise on DPOAE amplitude was determined at each of the 36 $L_1$-$L_2$ combinations, as schematized here (orange vs. blue in D). E,F: The resultant heat maps show the DPOAE amplitudes (E) averaged over the normalization window (blue box in D) and the change in DPOAE amplitude during contra-noise (F) for each $L_1$-$L_2$ combination. As a final metric of contra-sound effect for each ear, we measured the change in DPOAE from only the $L_1$-$L_2$ combinations eliciting maximal enhancement or suppression (stars in F).

Feeney and Keefe, 2001), except shifted to higher frequencies. Within the frequency band of maximal spectral difference (Fig. 5B, black box), the effect showed prominent post-onset adaptation with both a fast and a slow component (Fig. 5C), as has been observed in human reflexes elicited with high-pass contralateral noise (Djupesland et al., 1966). Growth functions measured before and after curare (Fig. 5D) suggested that the contra-noise effects were mediated exclusively by the MEMR.

Repeated, within-session measurements in a single subject (Fig. 6) suggested that reflex threshold and strength varied with anesthetic state. As shown in Fig. 6, the amplitude decreased and the threshold increased following the administration of boosters, and both slowly recovered over time. To try and minimize the effects of this variation in our measurements, attempts were made to gather data at stereotyped times with respect to anesthetic boosters.

One day post-exposure, reflex thresholds were ≥100 dB SPL in the neuropathic mice, i.e. at the limits of our acoustic system (not shown). By 1 wk post-exposure, when cochlear thresholds had returned to normal, reflex effects were once again measurable, though with reduced amplitude and elevated thresholds. Tests were repeated at 4 post-exposure times from 1 to 8 wks. A repeated measures analysis of variance indicated that there was no significant effect of time after exposure after cochlear thresholds had recovered (i.e. 1–8 wks post-exposure). Thus, we averaged data across all these measurement times (Fig. 7). In the neuropathic mice, the MEMR thresholds were permanently elevated (Fig. 7C) and the maximum amplitudes of the reflex effects were permanently reduced (Fig. 7E). The inter-group differences were statistically significant for both amplitude and threshold and for measures taken either at the onset and the offset of the contralateral noise.

## 4. Discussion

### 4.1. The MEMR can modulate DPOAEs in anesthetized mice

Modulation of ipsilateral responses by contralateral sound has long been used as an assay for either the MEMR or the MOCR in awake humans and in awake or anesthetized animals (Guinan, 2015). The extent to which each of the two reflexes contribute to this binaural effect depends on species, stimulus level and the type and level of anesthesia. In barbiturate-anesthetized cats (Puria et al., 1996) and guinea pigs (Kujawa and Liberman, 2001), the contra-noise effects are dominated by the MOCR. In contrast, in

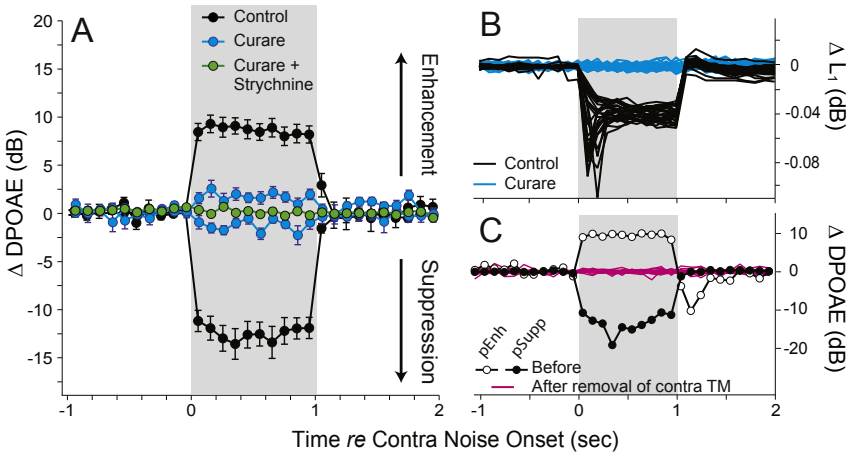


**Fig. 3.** Contra-noise modulation of high-level DPOAEs is dominated by the MEMR. A: Contra-noise effects on normalized DPOAE amplitudes ($f_2 = 32$ kHz) averaged over 3 trials per pharmacological manipulation in 6 control mice. For each condition, mean data are shown for two $L_1$-$L_2$ combinations: one showing maximal suppression, indicated in Fig. 2C, and one showing maximal enhancement, which was a few dB above notch center, as illustrated in Fig. 2F. Mean values (±SEM) are shown. B: Data from one ear showing contra-noise modulation of primary-tone level ($L_1$) in the ear canal in the 36 $L_1$-$L_2$ combinations of a 6 × 6 dB level matrix before (black) and after (cyan) curare injection. $f_2 = 32$ kHz, $L_1 = 90–95$ dB SPL (pre-curare) or 89–94 dB SPL (post-curare) and $L_2 = 83–88$ dB SPL. C: Data from one ear showing the changes in DPOAE amplitude before (black) and after (pink) removal of the contralateral TM. $f_2 = 32$ kHz. Before TM removal: $L_1/L_2 = 85/81$ dB SPL at peak enhancement (open circles) and $L_1/L_2 = 87/83$ dB SPL at peak suppression (filled circles). After TM removal: $L_1/L_2 = 84–89$ dB SPL (shifted up to surround the notch). For all panels, a 2-octave band noise centered at $f_2$ was presented contralaterally at 95 dB SPL (gray bar).

anesthetized rats (Relkin et al., 2005) and awake rabbits (Luebke et al., 2002; Whitehead et al., 1991), modulation of DPOAEs by contralateral noise is mediated primarily by the MEMR. In chinchillas, the MEMR- and MOCR-mediated suppression of DPOAEs can be separated by using a low- or high-frequency elicitor, respectively (Wolner et al., 2014). A previous study in ketamine/xylazine-anesthetized mice demonstrated that contra-noise suppression of low-level DPOAEs persisted following surgical or chemical lesion of the MOC pathway, following paralysis of the MEMs, and in mice lacking the nicotinic acetylcholine receptors necessary for MOC synaptic transmission (Maison et al., 2012). In contrast, the contra-noise modulation of high-level DPOAEs, i.e. around the notch of the amplitude vs. level function, was eliminated by the combined inactivation of the MEM and MOC reflexes. The current study replicated the latter finding and further demonstrated that it is actually the MEMR that dominates the modulation of high-level DPOAEs, i.e. the reflex strength was severely weakened following MEM paralysis alone. Thus, the effect of cochlear neuropathy on the strength of the MOC reflex remains an open question. Given that the variability and small size of the MOC effects in the present study (Fig. 4B) were likely due to anesthesia, the question will be best addressed in awake mice, where the MOC-mediated suppression DPOAEs is on the order of ~8–10 dB (Chambers et al., 2012). Here, we focus on the MEMR.

### 4.2. A simple model of sound-evoked drive to the MEMR

Since its introduction in the 1940s, MEMR tests have been widely applied in clinical diagnoses (see Silman, 1984, Thomsen, 1999 for reviews). Some MEMR assays have compared reflex thresholds elicited by narrow-vs. wide-band stimuli (Flottorp et al., 1971; Niemeyer and Sesterhenn, 1974; Jerger et al., 1974; Popelka et al., 1976), or by ipsilateral vs. contralateral stimuli (Mangham et al., 1970; Hall, 1982), and others have measured input/output functions (Silman and Gelfand, 1981) or the post-onset decay of reflex strength (Anderson et al., 1970; Cartwright and Lilly, 1976;

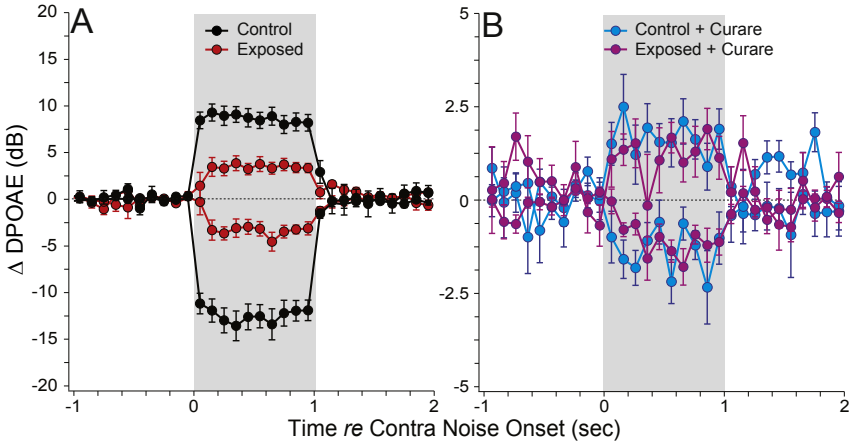


**Fig. 4.** Contra-noise modulation of DPOAEs is attenuated in neuropathic mice. A: Contra-noise effects on normalized DPOAE levels ($f_2 = 32$ kHz) in 6 control mice compared to 6 noise-exposed mice. Mean data (±SEMs) are shown: control data are the same as in Fig. 3A; exposed ears are from Group 1. In each ear, the $L_1/L_2$ combinations producing maximal enhancement or suppression were used for the averages, as described in Fig. 2F. B: Mean contra-noise effects from the same ears taken from level matrices focused around notch center, just as in A, but measured 15 min after injection of curare. Contra-noise was (12.8–51.2 kHz) at 95 dB SPL.

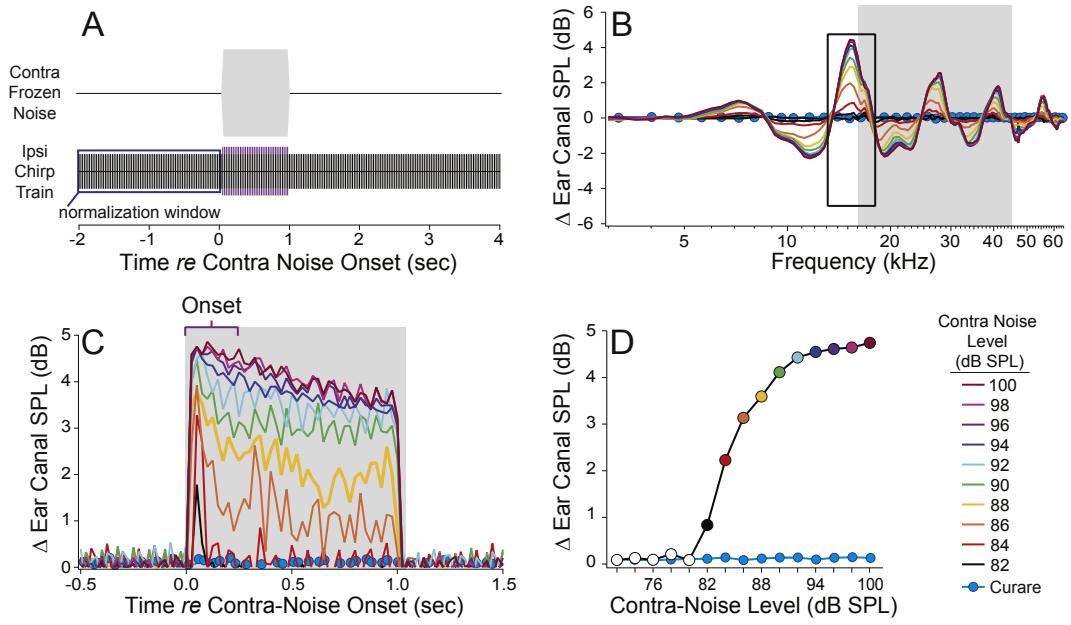


**Fig. 5.** Measuring contra-noise modulation of wideband reflectance. A: Schematic of the wideband contra-noise test, in which the ipsilateral stimulus is a 40-Hz train of 2-msec "chirps" (80 dB SPL), upswept from 4 to 64 kHz, and the contralateral reflex elicitor is a "frozen" high-pass noise (16–45.2 kHz), 1 s in duration (20-msec ramp), presented in alternating polarities every 6 sec. B: Ipsilateral ear-canal sound pressure waveform to each chirp was measured and fast Fourier transformed. The resultant spectra were averaged: one spectrum for chirps before contra-noise onset (blue box in A), and a second for chirps during contra-noise (purple lines in A). The difference between the two spectra, as shown here for a range of elicitor levels, was used to identify the frequency region of maximal effect (black box). C: Computing SPL within this frequency band, we plotted ear canal SPL as a function of time for each elicitor level, relative to the mean SPL before contra-noise onset. D: We collapsed the contra-noise effect at each elicitor level to a single number using a two-step process to maximize across time and frequency. First, using a frequency band spanning the positive-going deflection on the magnitude spectrum (black box in C), we found the three-point time window within the first 0.25 sec after contra-noise onset that maximized Δ Ear Canal SPL. Then, restricting analysis to this time window, we found the three consecutive frequency bins within the original frequency band that yielded the largest overall change in ear-canal SPL. Contra-noise effects were fully eliminated by curare (cyan filled circles in panels C–D).

see Wilson et al., 1984). Classically, the greatest diagnostic value of the MEMR test has been in the identification of retrocochlear pathology, i.e. auditory nerve dysfunction that is distinct from hair cell or other intracochlear pathology. Numerous studies have documented that MEMR threshold can be dramatically elevated or altogether absent in cases of VIIIth nerve tumors (Anderson et al., 1970; Cartwright and Lilly, 1976; Silman et al., 1978; see Wilson et al., 1984) and in patients with severe auditory neuropathy (Berlin et al., 2005, 2010). Conversely, MEMR thresholds for tonal stimuli can be normal or minimally elevated in sensorineural hearing loss with elevation of audiometric thresholds by ~40–60 dB (Popelka et al., 1976; Popelka, 1981) that is likely due to OHC damage.

Neurophysiological studies of stapedius motoneurons show exceedingly broad frequency tuning curves (FTCs) with thresholds similar to the broadly tuned, low-frequency "tails" of auditory nerve FTCs (Kobler et al., 1992). Similarly, MEMR thresholds for tonal stimuli, as measured in the ear canals of anesthetized rabbits, are similar in tuning and threshold to the low-frequency tails of ANFs (Borg et al., 1990). These results suggested that the circuitry driving the MEMR sums activity across ANFs from all cochlear regions and, once a threshold level is reached, sends a signal to the motoneuron pool that is proportional to this ensemble activity. Such a model is consistent with the observation that MEMR thresholds in humans decrease monotonically as the bandwidth of the elicitor stimulus is increased to cover more of the cochlear spiral (Margolis, 1993).

A variant of this model suggests that the afferent limb of the MEMR is dominated by high-threshold, low-SR ANFs (Liberman and Kiang, 1984; Roullier et al., 1986; Kobler et al., 1992). The

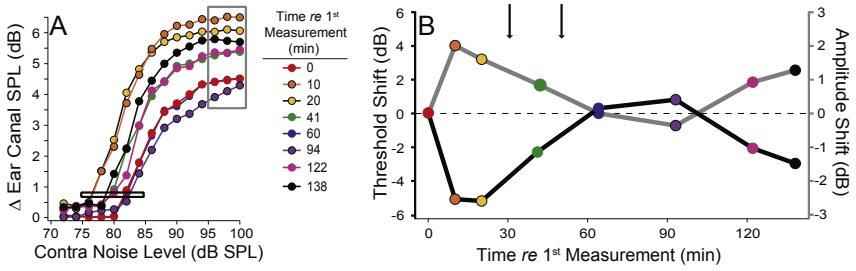


**Fig. 6.** Is the slow variation in contra-noise modulation of wideband reflectance related to anesthetic state? A: The change in wideband reflectance is shown as a function of increasing contra-noise level over repeated measurements within the same session in a single animal. B: Amplitudes (gray line, right axis) and thresholds (black line, left axis) for the contra-noise effect vary with time *re* anesthetic boosters (arrows). Threshold for this subject was defined as the contra-noise level required to produce a 0.75-dB change in reflectance (horizontal black rectangle in A); amplitude is the mean for contra-noise levels from 96 to 100 dB SPL (vertical gray box in A). Data were normalized to the first measurement, which was 38 min following induction of anesthesia.

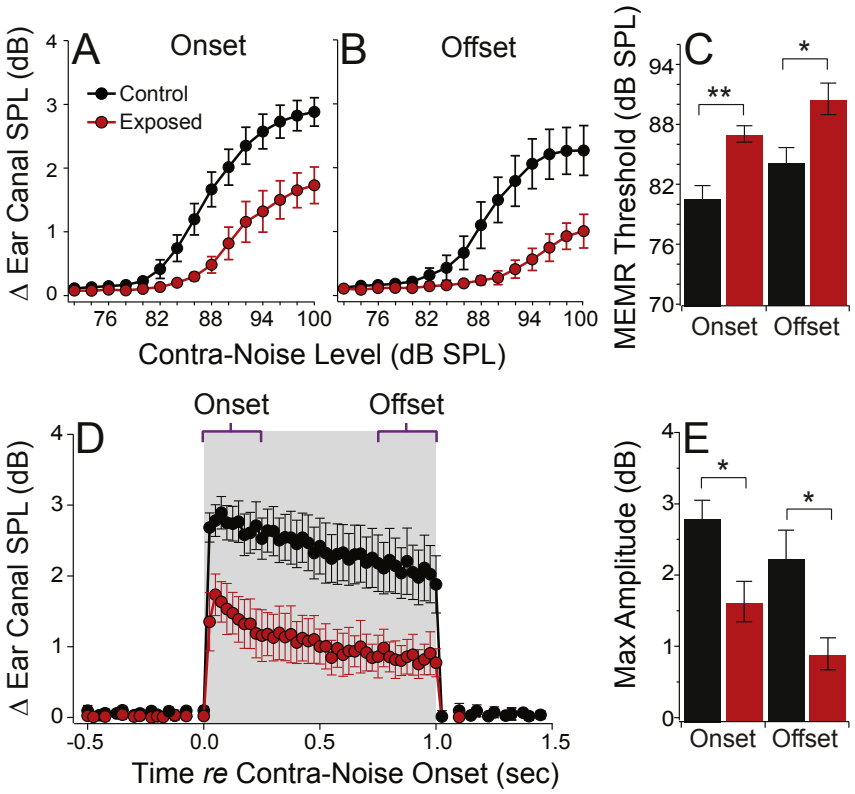


**Fig. 7.** The MEMR is attenuated in mice with cochlear neuropathy. Contra-noise effects on wideband reflectance are shown for 4 control and 4 noise-exposed animals (Group 2) averaged over 4 repeated measures between 1 and 8 wk post-noise exposure. A,B: Growth functions of the MEMR are shown at contra-noise onset (A), as described in Fig. 5, and at contra-noise offset (B), with the time window in Fig. 5C moved to the final 0.25 sec of the contra-noise presentation. C: Mean "threshold" for the MEMR for same ears, defined as the lowest stimulus level producing a response greater than 3 standard deviations above the mean noise floor of all trials. D: Mean effects on ipsilateral ear-canal SPL from a 100 dB SPL contra noise for the control vs. exposed ears, extracted as described for Fig. 5C. E: Mean maximum amplitude of contra-noise suppression at onset and offset for the two experimental groups, defined as the average of the response amplitude for contra-noise elicitors at 96–100 dB SPL. Error bars in all panels represent ±1 SEM. Asterisks indicate statistical significance: * for $P < 0.05$; ** for $P < 0.01$.

suggestion is based on two observations about low-SR physiology: 1) in normal ears, the tone-evoked discharge rate in the low-frequency tails of low-SR fibers increases very rapidly at SPLs near 85 dB SPL, which is similar to the MEMR thresholds for tones, and 2) this high-level "component" of the low-SR response is extremely resistant to cochlear damage (Liberman and Kiang, 1984).

### 4.3. Cochlear pathophysiology and its effects on the audiogram vs. the MEMR

Regardless of whether the MEMR is driven by all ANFs or only a subset, it is useful to consider what this simple model predicts about the MEMR with different etiologies of sensorineural hearing loss (SNHL). Neurophysiological studies of noise-induced (Furman et al., 2013), drug-induced (Lobarinas et al., 2013) or age-related (Sergeyenko et al., 2013) hearing loss suggest general principles about the relationship between auditory nerve pathophysiology and cochlear histopathology that are useful in thinking about the MEMR in SNHL.

The OHCs are among the most vulnerable cells in the cochlea (Johnson and Hawkins, 1972; Bohne and Harding, 2000). With pure OHC loss, auditory nerve FTCs have attenuated "tips" and slightly hypersensitive "tails," while dynamic range (typically 20–30 dB) and maximum discharge rate remain unchanged (Liberman and Kiang, 1978). Thus, a pure OHC lesion should leave the MEMR unaffected, despite threshold elevation of up to 50 dB, as is often observed (Metz, 1946; Jerger et al., 1978; Hyde et al., 1980; Popelka, 1981; Margolis, 1993), since the ensemble ANF discharge to tones > 80 SPL should not be different from normal.

IHC loss can be induced with carboplatin in chinchillas (e.g., Harrison, 1998; Lobarinas et al., 2013) and is often observed in premature infants (Amatuzzi et al., 2001). Diffuse IHC loss will not affect audiometric thresholds until the loss exceeds 80% (Lobarinas et al., 2013) and OAEs can remain unchanged (Liberman et al., 1997). However, IHC loss will decrease the suprathreshold ensemble discharge rate in ANFs in direct proportion to fractional IHC loss, and thus should raise MEMR thresholds more than audiometric thresholds, as seen for VIIIth nerve tumors. Damage to IHC stereocilia, as often occurs in noise-induced hearing loss, can also elevate single fiber thresholds, including the tails of the FTCs (e.g., Liberman and Kiang, 1984; Liberman and Dodds, 1984). Thus, in some cases, noise exposure can significantly elevate both MEMR thresholds and audiometric thresholds, as has been observed in rabbits with significant damage to IHC stereocilia (Engstrom and Borg, 1983).

Recent work on noise-induced and age-related hearing loss shows that the synapses between ANFs and IHCs are the most vulnerable elements in the inner ear (e.g., Kujawa and Liberman, 2009). Since each spiral ganglion neuron contacts a single IHC by a single synapse, each missing synapse in a noise-exposed or aging ear corresponds to an ANF that has lost all response to sound. Thus, the elevation of MEMR threshold and reduction in suprathreshold MEMR reflex strength observed here in our neuropathic mice is consistent with the simple MEMR model. In most types of SNHL, the damage is a complicated mixture of OHC and IHC loss and

damage (Liberman and Dodds, 1984), along with the degeneration of synaptic contacts on surviving IHCs (Kujawa and Liberman, 2009). Therefore, it is not surprising that there are no general rules relating threshold shift (commonly referred to as "hearing loss") and MEMR threshold.

The neuropathic model tested here is useful because there is no permanent hearing threshold shift to confound interpretation. Any changes in ANF output are caused only by synaptopathy and not by OHC damage. The present results help explain how MEMR thresholds could be significantly elevated in mild hearing loss (Keith, 1977; Alberti and Kristensen, 1970; Jerger et al., 1974; Silman et al., 1978; Popelka, 1981). Furthermore, the observation that the elicitor-bandwidth effect, i.e. the lowering of MEMR threshold with increasing elicitor bandwidth, is reduced in aged listeners with normal hearing sensitivity (Margolis, 1993) is consistent with the presence of cochlear neuropathy in the absence of hair cell loss, as has recently been reported in a human temporal-bone study (Viana et al., 2015).

### 4.4. MEMRs in the diagnosis of cochlear neuropathy

Using the standard tonal probe at 220 Hz, a weakened MEMR can be seen in humans with noise-induced hearing loss with an elicitor at a frequency within a patient's "normal" audiometric range (Houghton et al., 1988). However, it may be preferable to use a frequency glide, or chirp, for the probe. The human MEMR threshold can be reduced by up to 24 dB by using a wideband vs. a tonal probe (Feeney and Keefe, 2001). If, as current data suggest, neuropathic patients are vulnerable to further cochlear damage due to a weakened MEMR, high-intensity reflex elicitors, i.e. >100 dB SPL, may be contraindicated. Indeed, there have been cases in which MEMR tests were reported to cause temporary and permanent threshold shifts (see Schairer et al., 2013). The addition of the wideband acoustic reflex test also may be a useful addition to newborn screening programs (Keefe et al., 2010), particularly for premature or otherwise at-risk infants (e.g., Amatuzzi et al., 2001), as it does not require the pressurization of the ear canal (Schairer et al., 2007), and it may aid in the identification of more moderate pathologies than can be detected by the ABR.

Contamination of MEMR measurements by the MOCR could be minimized with careful parameter choices. For example, the magnitude of the MOC-mediated effect will be miniscule in comparison with the MEM-mediated effect if the chirp is presented at a relatively high level (60–80 dB SPL: Guinan et al., 2003). Unfortunately to date, the published literature examining MEMR in subjects with sensorineural hearing loss includes only tonal probes. In order to improve its utility in differential diagnostics, there is a need to examine the effects of various cochlear pathologies on the wideband MEMR.

## Acknowledgments

We thank Christopher Shera and John Guinan for aid in experimental design, and John Guinan for reviewing an earlier version of this manuscript. We also thank Leslie Liberman for expert assistance in cochlear dissection and immunostaining for a subset of the cochleas. Research supported by grants from the National Institute on Deafness and other Communicative Disorders: R01 DC 00188 (MCL), P30 DC 05209 (MCL), and F32 DC 014405 (MDV).

## References

Alberti, P.R., Kristensen, R., 1970. The clinical application of impedance audiometry. Laryngoscope 80, 735–746.

Amatuzzi, M.G., Northrop, C., Liberman, M.C., Thornton, A., Halpin, C., Herrmann, B., Pinto, L.E., Saenz, A., Carranza, A., Eavey, R.D., 2001. Selective inner hair cell loss in premature infants and cochlea pathological patterns from neonatal intensive care unit autopsies. Arch. Otolaryngol. Head Neck Surg. 127, 629–636.

Anderson, H., Barr, B., Wedenberg, E., 1970. The early detection of acoustic tumours by the stapedius reflex test. In: Wolstenholme, G.E.W., Knight, J., Churchill, A. (Eds.), Sensorineural Hearing Loss, pp. 275–294. London.

Berlin, C.I., Hood, L.J., Morlet, T., Wilensky, D., Mattingly, K.R., Taylor-Jeanfreau, J., Keats, B.J.B., St John, P., Montgomery, E., Shallop, J.K., Russell, B.A., Frisch, S.A., 2010. Multi-site diagnosis and management of 260 patients with auditory neuropathy/dys-synchrony (auditory neuropathy spectrum disorder*). Int. J. Audiol. 49, 30–43.

Berlin, C.I., Hood, L.J., Morlet, T., Wilensky, D., St John, P., Montgomery, E., Thjibodaux, M., 2005. Absent or elevated middle ear muscle reflexes in the presence of normal otoacoustic emissions: a universal finding in 136 cases of auditory neuropathy/dys-synchrony. J. Am. Acad. Audiol. 16, 546–553.

Bohne, B.A., Harding, G.W., 2000. Degeneration in the cochlea after noise damage: primary versus secondary events. Am. J. Oto 21, 505–509.

Borg, E., 1966. A quantitative study of the effect of the acoustic stapedius reflex on sound transmission through the middle ear of man. Acta-Otolaryngol 66, 461–472.

Borg, E., Counter, A.S., Engstrom, B., Linde, G., Marklund, K., 1990. Stapedius reflex thresholds in relation to tails of auditory nerve fiber frequency tuning curves. Brain Res. 506, 79–84.

Cartwright, D., Lilly, D., 1976. A Comparison of Acoustic Reflex Decay Patterns for Patients with Cochlear and VIIIth-nerve Disease. American Speech-Language-Hearing Association Convention, Houston.

Chambers, A.R., Hancock, K.E., Maison, S.F., Liberman, M.C., Polley, D.B., 2012. Sound-evoked olivocochlear activation in unanesthetized mice. J. Assoc. Res. Otolaryngol. 13, 209–217.

Collet, L., Kemp, D.T., Veuillet, E., Duclaux, R., Moulin, A., Morgon, A., 1990. Effect of contralateral auditory stimuli on active cochlear micro-mechanical properties in human subjects. Hear. Res. 43, 251–262.

Costalupes, J.A., Young, E.D., Gibson, D.J., 1984. Effects of continuous noise backgrounds on rate response of auditory nerve fibers in cat. J. Neurophysiol. 51, 1326–1344.

Djupesland, G., Flottorp, G., Winther, F., 1966. Size and duration of acoustically elicited impedance changes in man. Acta Oto-laryngol (Suppl. 224), 220–228.

Elgoyhen, A.B., Johnson, D.S., Boulter, J., Vetter, D., Heinemann, S., 1994. α9: an acetylcholine receptor with novel pharmacologic properties expressed in rat cochlear hair cells. Cell 79, 705–715.

Elgoyhen, A.B., Vetter, D.E., Katz, E., Rothlin, C.V., Heinemann, S.F., Boulter, J., 2001. Alpha10: a determinant of nicotinic cholinergic receptor function in mammalian vestibular and cochlear mechanosensory hair cells. Proc. Natl. Acad. Sci. U. S. A. 98, 3501–3506.

Engstrom, B., Borg, E., 1983. Cochlear morphology in relation to loss of behavioural, electrophysiological, and middle ear reflex thresholds after exposure to noise. Acta Otolaryngol. (Suppl. 402), 3–23.

Feeney, M.P., Keefe, D.H., 2001. Estimating the acoustic reflex threshold from wideband measures of reflectance, admittance, and power. Ear Hear 22, 316–332.

Feeney, M.P., Keefe, D.H., Marryott, L.P., 2003. Contralateral acoustic reflex thresholds for tonal activators using wideband reflectance and admittance measurements. J. Speech Lang. Hear. Res. 46, 128–136.

Feeney, M.P., Keefe, D.H., Sanford, C.A., 2004. Wideband reflectance measures of the ipsilateral acoustic stapedius reflex threshold. Ear. Hear. 25, 421–430.

Flottorp, G., Djupesland, G., Winther, F., 1971. The acoustic stapedius reflex in relation to critical bandwidth. J. Acoust. Soc. Am. 49 (Suppl. 2), 427–461.

Furman, A.C., Kujawa, S.G., Liberman, M.C., 2013. Noise-induced cochlear neuropathy is selective for fibers with low spontaneous rates. J. Neurosci. 110, 577–586.

Gelfand, S.A., Piper, N., 1981. Acoustic reflex thresholds in young and elderly subjects with normal hearing. J. Acoust. Soc. Am. 69, 295–297.

Gelfand, S.A., Piper, N., Silman, S., 1983. Effects of hearing levels at the activator and other frequencies upon the expected levels of the acoustic reflex threshold. J. Speech Hear. Dis. 48, 11–17.

Gorga, M.P., Kaminski, J.R., Beauchaine, K.A., Jesteadt, W., 1988. Auditory brainstem responses to tone bursts in normally hearing subjects. J. Speech. Hear. Res. 31, 87–97.

Guinan Jr., J.J., 2006. Olivocochlear efferents: anatomy, physiology, function, and the measurement of efferent effects in humans. Ear. Hear 27, 589–607.

Guinan Jr., J.J., 2015. Olivocochlear efferent function: issues regarding methods and the interpretation of results. Front. Syst. Neurosci. 8 (142), 1–5.

Guinan Jr., J.J., Backus, B.C., Lilaonitkul, W., Aharonson, V., 2003. Medial olivocochlear efferent reflex in humans: otoacoustic emission (OAE) measurement issues and the advantages of stimulus frequency OAEs. J. Assoc. Res. Otolaryngol. 4, 521–540.

Houghton, J.M., Greville, K.A., Keith, W.J., 1988. Acoustic reflex amplitude and noise-induced hearing loss. Audiology 27, 42–48.

Hyde, M.L., Alberti, P.W., Morgan, P.P., Symons, F., Cummings, F., 1980. Pure-tone threshold estimation by acoustic reflex thresholds – a myth? Acta Otolaryngol. 89, 345–357.

Jerger, J., Hurney, P., Mauldin, L., Crump, B., 1974. Predicting hearing loss from the acoustic reflex. J. Speech Hear. 19, 11–22. Dis.

Jerger, J., Hayes, D., Anthony, L., Mauldin, L., 1978. Factors influencing prediction of

hearing level from the acoustic reflex. Monogr. Contemp. Audiol. 1, 1–20.
Johnson, L.G., Hawkins Jr., J.E., 1972. Sensory and neural degeneration with aging as seen in microdissections of the human inner ear. Ann. Otol. Rhinol. Laryngol. 81, 179–193.
Kawase, T., Delgutte, B., Liberman, M.C., 1993. Antimasking effects of the olivocochlear reflex. II. Enhancement of auditory-nerve response to masked tones. J. Neurophysiol. 70, 2533–2549.
Keefe, D.H., Ling, R., Bulen, J., 1992. Method to measure acoustic impedance and reflection coefficient. J. Acoust. Soc. Am. 91, 470–485.
Keith, R.W., 1977. An evaluation of predicting hearing loss from the acoustic reflex. Arch. Otolaryngol. 103, 419–424.
Kobler, J.B., Guinan Jr., J.J., Vacher, S.R., Norris, B.E., 1992. Acoustic reflex frequency selectivity in single stapedius motoneurons of the cat. J. Neurophysiol. 68, 807–817.
Kujawa, S.G., Liberman, M.C., 2001. Effects of olivocochlear feedback on distortion product otoacoustic emissions in guinea pig. J. Assoc. Res. Otolaryngol. 2, 268–278.
Kujawa, S.G., Liberman, M.C., 2006. Acceleration of age-related hearing loss by early noise exposure: evidence of a misspent youth. J. Neurosci. 26, 2115–2123.
Kujawa, S.G., Liberman, M.C., 2009. Adding insult to injury: cochlear nerve degeneration after “temporary” noise-induced hearing loss. J. Neurosci. 29, 14077–14085.
Kujawa, S.G., Liberman, M.C., 2015. Synaptopathy in the noise-exposed and aging cochlea: primary neural degeneration in acquired sensorineural hearing loss. Hear. Res. http://dx.doi.org/10.1016/j.heares.2015.02.009 [E-pub ahead of print].
Liberman, M.C., 1988. Physiology of cochlear efferent and afferent neurons: direct comparisons in the same animal. Hear. Res. 34, 179–191.
Liberman, M.C., 1991. Central projections of auditory-nerve fibers of differing spontaneous rate. I. Anteroventral cochlear nucleus. J. Comp. Neurol. 313, 240–258.
Liberman, M.C., Chesney, C.P., Kujawa, S.G., 1997. Effects of selective inner hair cell loss on DPOAE and CAP in carboplatin-treated chinchillas. Aud. Neurosci. 3, 255–268.
Liberman, M.C., Dodds, L.W., 1984. Single-neuron labeling and chronic cochlear pathology. II. Stereocilia damage and alterations of spontaneous discharge rates. Hear. Res. 16, 43–53.
Liberman, M.C., Kiang, N.Y.S., 1978. Acoustic trauma in cats, cochlear pathology and auditory-nerve activity. Acta Otolaryngol. (Suppl. 358), 1–63.
Liberman, M.C., Kiang, N.Y.S., 1984. Single-neuron labeling and chronic pathology. IV. Stereocilia damage and alterations in rate and phase level functions. Hear. Res. 16, 75–90.
Liberman, M.C., Suzuki, J., Liberman, L.D., 2015. Dynamics of cochlear synaptopathy after acoustic overexposure. J. Assoc. Res. Otolaryngol. 16, 205–219.
Lobarinas, E., Salvi, R., Ding, D., 2013. Insensitivity of the audiogram to carboplatin induced inner hair cell loss in chinchillas. Hear. Res. 302, 113–120.
Luebke, A.E., Foster, P.K., Stagner, B.B., 2002. A multifrequency method for determining cochlear efferent activity. J. Assoc. Res. Otolaryngol. 3, 16–25.
Maison, S.F., Usubuchi, H., Vetter, D.E., Elgoyhen, A.B., Thomas, S.A., Liberman, M.C., 2012. Contralateral-noise effects on cochlear responses in anesthetized mice are dominated by feedback from an unknown pathway. J. Neurophysiol. 108, 491–500.
Margolis, R.H., 1993. Detection of hearing impairment with the acoustic stapedius reflex. Ear Hear 14, 3–10.
McMillan, P.M., Bennett, M.J., Marchant, C.D., et al., 1985. Ipsilateral and contralateral acoustic reflexes in neonates. Ear. Hear 6, 320–324.
Metz, O., 1946. The acoustic impedance measured on normal and pathological ears. Acta Otolaryngol. (Suppl. 63), 1–254.
Neimeyer, W., Sesterhenn, G., 1974. Calculating the hearing threshold from the stapedius reflex threshold for different sound stimuli. Audiol 13, 421–427.
Neumann, J., Uppenkamp, S., Kollmeier, B., 1994. Chirp evoked otoacoustic emissions. Hear. Res. 79, 17–25.
Nikiforidis, G.C., Koutsojannis, C.M., Varakis, J.N., Goumas, P.D., 1993. Reduced variance in the latency and amplitude of the fifth wave of auditory brain stem response after normalization for head size. Ear Hear 14, 423–428.
Pang, X.D., Guinan Jr., J.J., 1997. Effects of stapedius-muscle contractions on the masking of auditory-nerve responses. J. Acoust. Soc. Am. 102, 3576–3586.
Plack, C.J., Barker, D., Prendergast, G., 2014. Perceptual consequences of “hidden” hearing loss. Trends hear.. 18, 1–11.
Popelka, G.R. (Ed.), 1981. Hearing Assessment with the Acoustic Reflex (New York Grune & Stratton).
Popelka, G.R., Margolis, R.H., Wiley, T.L., 1976. Effect of activating signal bandwidth on acoustic-reflex thresholds. J. Acoust. Soc. Am. 59, 154–159.
Puria, S., Guinan Jr., J.J., Liberman, M.C., 1996. Olivocochlear reflex assays: effects of contralateral sound on compound action potentials vs. ear-canal distortion products. J. Acoust. Soc. Am. 99, 500–507.
Rajan, R., 1995. Involvement of cochlear efferent pathways in protective effects elicited with binaural loud sound exposure in cats. J. Neurophysiol. 74, 582–597.
Reiter, E.R., Liberman, M.C., 1995. Efferent-mediated protection from acoustic overexposure: relation to slow effects of olivocochlear stimulation. J. Neurophysiol. 73, 506–514.
Relkin, E.M., Sterns, A., Zeredo, W., Prieve, B.A., Woods, C.I., 2005. Physiological mechanisms of onset adaptation and contralateral suppression of DPOAEs in the rat. J. Assoc. Res. Otolaryngol. 6, 119–135.
Rosowski, J.J., Stenfelt, S., Lilly, D., 2013. An overview of wideband immitance measurement techniques and terminology: you say absorbance, I say reflectance. Ear Hear 34, 9S–16S.
Rothlin, C.V., Katz, E., Verbitsky, M., Elgoyhen, A.B., 1999. The alpha9 nicotinic acetylcholine receptor shares pharmacological properties with type A gamma-aminobutyric acid, glycine, and type 3 serotonin receptors. Mol. Pharmacol. 55, 248–254.
Rouiller, E.M., Cronin-Schreiber, R., Fekete, D.M., Ryugo, D.K., 1986. The central projections of intracellularly labeled auditory nerve fibers in cats: an analysis of terminal morphology. J. Comp. Neurol. 249, 261–278.
Ruan, Q., Ao, H., He, J., Chen, Z., Yu, Z., Zhang, R., Wang, J., Yin, S., 2014. Topographic and quantitative evaluation of gentamicin induced damage to peripheral innervation of mouse cochlea. Neurotoxicol 40, 86–96.
Schaette, R., McAlpine, D., 2011. Tinnitus with a normal audiogram: physiological Evidence for hidden hearing loss and computational model. J. Neurosci. 31, 13452–13457.
Schairer, K.S., Ellison, J.C., Fitzpatrick, D.F., Keefe, D.H., 2007. Wideband ipsilateral measurements of middle-ear muscle reflex thresholds in children and adults. J. Acoust. Soc. Am. 121, 3607–3616.
Schairer, K.S., Feeney, M.P., Sanford, C.A., 2013. Acoustic reflex measurement. Ear Hear. 34 (Suppl. 1), 43–47.
Schuknecht, H.F., Woellner, R.C., 1955. An experimental and clinical study of deafness from lesions of the cochlear nerve. J. Laryngol. Otol. 69, 75–97.
Sergeyenko, Y., Lall, K., Liberman, M.C., Kujawa, S.G., 2013. Age-related cochlear synaptopathy: an early-onset contributor to auditory functional decline. J. Neurosci. 21, 13686–13694.
Shaheen, L.A., Valero, M.D., Liberman, M.C., 2015. Toward a diagnosis of cochlear neuropathy with envelope following responses. J. Assoc. Res. Otolaryngol. 16, 727–745.
Silman, S., Popelka, G.R., Gelfand, S.A., 1978. Effect of sensorineural hearing loss on acoustic stapedius reflex growth function. J. Acoust. Soc. Am. 64, 1406–1411.
Silman, S., Gelfand, S.A., 1981. Effect of sensorineural hearing loss on the stapedius reflex growth function in the elderly. J. Acoust. Soc. Am. 69, 1099–1106.
Simmons, F.B., 1960. Middle ear muscle protection from the acoustic trauma of loud continuous sound. Ann. Otol. Rhinol. Laryngol. 72, 528–548.
Sridhar, T.S., Liberman, M.C., Brown, M.C., Sewell, W.F., 1995. A novel cholinergic “slow effect” of efferent stimulation on cochlear potentials in the guinea pig. J. Neurosci. 15, 3667–3678.
Viana, L.M., O'Malley, J.T., Burgess, B.J., Jones, D.D., Oliviera, C.A.C.P., Santos, F., Merchant, S.N., Liberman, L.D., Liberman, M.C., 2015. Cochlear neuropathy in human presbycusis: confocal analysis of hidden hearing loss in post-mortem tissue. Hear. Res. 327, 78–88.
Wan, G., Gómez-Casati, M.E., Gigliello, A.R., Liberman, M.C., Corfas, G., 2014. Neurotrophin-3 regulates ribbon synapse density in the cochlea and induces synapse regeneration after acoustic trauma. Elife (3), e03564.
Wang, Y., Ren, C., 2012. Effects of repeated “benign” noise exposures in young CBA mice: shedding light on age-related hearing loss. J. Assoc. Res. Otolaryngol. 13, 505–515.
Whitehead, M.L., Martin, G.K., Lonsbury-Martin, B.L., 1991. Effects of the crossed acoustic reflex on distortion-product otoacoustic emissions in awake rabbits. Hear. Res. 51, 55–72.
Wilson, R.H., Shanks, J.E., Lilly, D.J., 1984. Acoustic-reflex adaptation. In: Silman, S. (Ed.), The Acoustic Reflex: Basic Principles and Clinical Applications. Academic Press, Inc, Orlando, Florida.
Wolter, N.E., Harrison, R.V., James, A.L., 2014. Separating the contributions of olivocochlear and middle ear muscle reflexes in modulation of distortion product otoacoustic emission levels. Audiol. Neurootol 19, 41–48.
Ye, Y., Machado, D.G., Do, K., 2000. Projection of the marginal shell of the anteroventral cochlear nucleus to olivocochlear neurons in the cat. J. Comp. Neurol. 420, 127–138.